Dynamic adsorbate/reaction induced structural change of supported metal nanoparticles: heterogeneous catalysis and beyond

Mark A. Newton*

Received 1st May 2008
First published as an Advance Article on the web 9th October 2008
DOI: 10.1039/b707746g

Our ever advancing abilities to examine nanosize metals and/or oxides with atomic and/or high temporal resolution have recently started to reveal much that is new about the behaviour of such systems. In many cases the notion of passive entities, upon which catalytic events occur, has been overturned, and with it many ideas that for a long time were axiomatic to the understanding of their behaviour. In its place a world of structuro-reactive dynamism is starting to appear wherein the atomic scale structure and reactivity are intimately tied to the nature of the environment being experienced. The aim of this *tutorial review* is to introduce the reader to these phenomena, to discuss how we might observe and categorise differing types of dynamic change, and to give some specific examples of where and how this fundamental structural dynamism can be tangibly linked to the reactive behaviour of heterogeneous catalysts.

Introduction

Metal nanoparticles in a variety of circumstances, and by virtue of their specific physical or chemical properties, are central to an enormous range of processes and technologies of industrial and economic importance. As components of heterogeneous catalysts they are supported upon a range of high area materials such as, for example, inorganic oxides or high area carbons. In this state they catalyse a plethora of important reactions—from cleaning up car exhaust emissions or producing electrical energy in fuel cells, to refining crude oil stocks and synthesising the raw feedstocks for yet further catalytic processes.

Such supported metal nanoparticles have been, and continue to be, the subject of intense research at many levels. Implicit in much of this research, historically speaking, is the notion of metallic particles upon which the catalysis, or at least part of the overall process at hand, occurs: the metal particle itself is viewed as a relatively invariant conduit for the desired chemistry. One could say that this axiom has underpinned much fundamental Ultra High Vacuum (UHV) based study of the chemistry of gases adsorbed upon well defined metal surfaces. Whilst in some cases impressive, and quantitative, explanations of some processes have resulted from UHV studies of low index, single crystal surfaces[1,2] it is clear that in many cases this notion is at best incomplete.[2]

Amongst the potential candidates for explaining the shortcomings of a "static" metal particle model of a complex material like a catalyst is simply that, in some structural-reactive way, the nanoparticle is a fluid entity that can rapidly change its habit or phase according to its environment; and that this might be in some way deterministic, for better or worse, in terms of the process being mediated. Even in the rarified world of UHV single crystal metal studies the potential for a reactive structural fluidity (*via* adsorbate induced surface reconstruction) has long been known.

Evidence that a panopoly of other such "form altering" processes may exist in the world of supported metal nanoparticles has also been with us for some time: the volatilisation of Ni as toxic $Ni(CO)_4$ has long been known and utilised as a central step in the Mond process;[3] 50 years ago infrared spectroscopy (IR) provided evidence that, in the presence of CO, supported Rh nanoparticles may transmute into a supported $Rh^{I}(CO)_2$ species;[4] and at least 40 years ago it became clear that, for the most part, deactivation of noble metal based catalysts used for hydrocarbon reforming and auto-exhaust processes was due to loss of active metal surface area (sintering) through particle growth resulting from the thermal and chemical rigours of these applications.[5] Indeed, undoing the effects of particle sintering, *via* "oxidative redispersion" has long been an important process in the petrochemical industry for reactivation of spent catalysts.[6]

Despite this, the detailed nature and timescales of such structural change have remained, in general, far from clear.

The European Synchrotron Radiation Facility, 6, Rue Jules Horowitz, BP-220, F-38043 Grenoble, France. E-mail: newton@esrf.fr; Fax: 00 33 (0)476 88 2784; Tel: +33 (0)476 88 2809

Mark Newton

Mark Newton received a degree in Chemistry and a PhD in Surface science from the University of Liverpool, UK. He has subsequently worked at the Universities of Washington, Seattle, USA and Southampton, UK. He is currently a beamline scientist (ID24 – Dispersive EXAFS) at the European Synchrotron Radiation Facility (ESRF), Grenoble, France and is a visiting scientist in the Department of Chemistry, University of Reading, UK.

Thus their potential importance in determining the overall behaviour of a catalyst in a given situation remains poorly understood. However, developments in a number of areas are starting to allow us to see inside catalyst behaviour with ever greater temporal and structural-reactive resolution. What is starting to emerge in many cases is that supported metal nanoparticles are often far from structurally passive: indeed, very rapid changes in form or phase often appear integral to the conditions they experience and processes they mediate.

This article aims to provide an introduction to some of the structuro-reactive behaviour that supported metal nanoparticles can display, how we might observe and quantify them on the timescales that they occur, and how these nanoscale phenomena might be correlated to aspects of their catalytic behaviour. Further, whilst this article is couched in the realm of heterogeneous catalysis, it is worth noting that many other properties (for instance, magnetic, optical, bactericidal, and biocompatibility) of metal nanoparticles, and the practical applications that arise from them, will also be dependent to a greater or lesser degree upon their precise form and how that form may be maintained under the conditions in which they are applied.

What types of structural change might occur and why should they interest us?

Why should these phenomena be important? Firstly, it is clear that differing phases (for instance, metallic, oxidic, organometallic) are liable to have very different physical and chemical properties. Thus, one really needs to know which phase is best suited to mediating a given process, and how to maximise the fraction of the metal component in the desired phase under the reaction conditions. An understanding of how different phases are produced or interconverted is therefore a key factor in any rational approach to catalyst design.

Fig. 1 shows a generalised schematic representing types of alteration that a metal nanoparticle might be foreseen to undergo in response to interacting with a reactive phase.

These might be divided into two broad groups: in the first the native internal structure (fcc, bcc, hcp) remains intact but the particles reorganise in response to a physical or chemical stimulus. As a result they may change size (sinter/disperse) and/or shape (refacet/flatten). In the second grouping a reactive event induces changes of phase (*e.g.* oxidation, or oxidative disruption to yield organometallic species) in the metal.

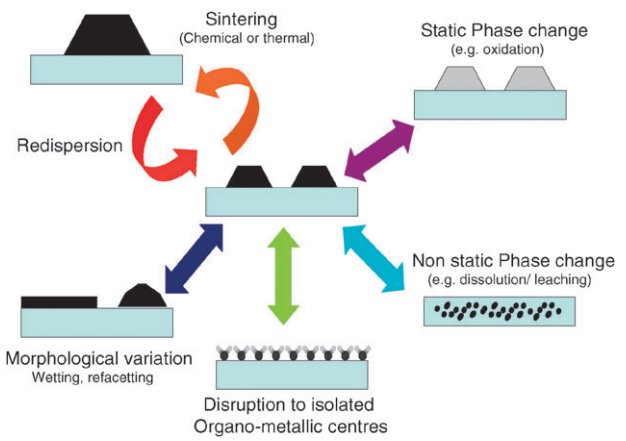

Fig. 1 Some schematic examples of structural changes that supported metal nanoparticles might undergo in response to physical or chemical stimuli, such as changes in temperature and/or reactive environment.

A priori there is no reason why events of differing types might occur together or as a consequence of another event. A change of phase (to, for example, an oxide) may subsequently trigger a change of morphology; or a change in size will result in a different optimal shape and facetting arrangement. Thus a considerable array of combinations of reactive structural change is potentially possible. Even if a supported metal keeps its intrinsic internal structure, and only changes size or shape, changes to reactive chemistry can be expected in the nano regime (see below).

The underlying factors that determine what might occur are thermodynamic, and the overall driving force for any reactive change will be that which best lowers the total energy of the system. An extensive discussion of this is well beyond the scope of this review and for an in depth study of the thermodynamics of adsorption of metals upon oxide surfaces the reader is referred elsewhere.[7] For the purposes of this review, however, it is sufficient to say that this is a multiparametric problem wherein a number of physical variables—that are often in themselves size dependent—are at work and competing with each other: for instance, the cohesive energy of the metal particle; the particle surface free energy; the heat of adsorption of the metal on the support material; and the heat of adsorption/reaction and the coverage of any species interacting with the metal nanoparticle.

Fig. 2 shows how the cohesive energy of some important metals is calculated to vary as a function of the number of atoms in a particle.[8] It is clear that in each case, below a certain particle size, a significant decrease in the cohesive energy of the particle is predicted. To a first approximation, therefore, one would predict that, as this starts to happen, the

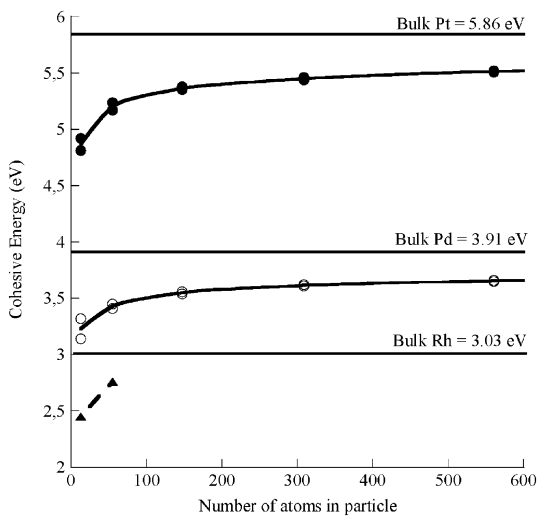

Fig. 2 Variation of particle (icosahedral and cubooctahedral) cohesive energies as a function of number of metal atoms, for three catalytically important noble metals: Pt (solid circles), Pd (open circles) and Rh (triangles). The bulk cohesive energies are also indicated. After Bazin and reproduced with permission from ref. 8.

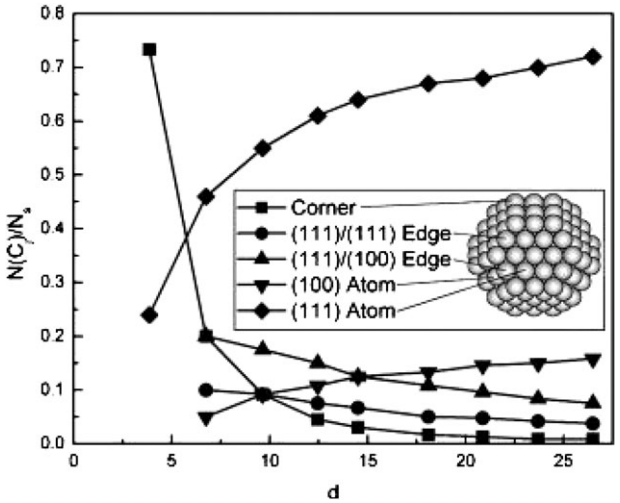

Fig. 3 Distribution of metal atoms at corner, edge, and plane sites divided by the total number of surface atoms as a function of the relative diameter of the nanoparticle. Reproduced with permission from ref. 9.

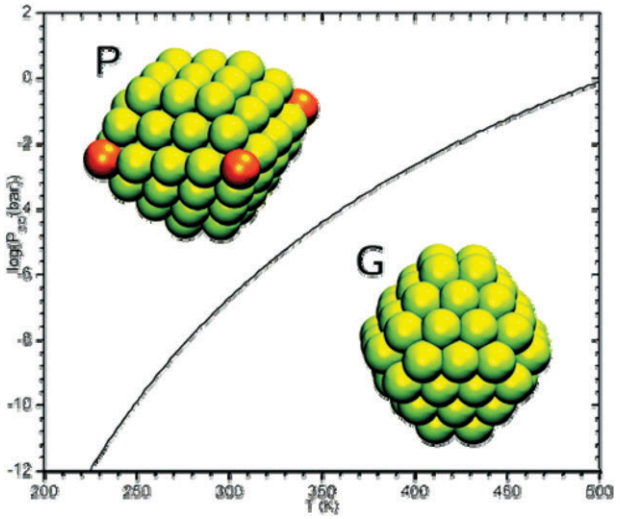

Fig. 4 Calculated phase diagram ($P_{(CO)}$ *vs.* T (K)) indicating the preferred morphology of free Au_{79} particles as a function of partial pressure of CO. CO rearranges the particle to expose more four-co-ordinate (red) Au sites, flattening the particle and decreasing the net Au co-ordination number. Reproduced with permission from ref. 16.

potential for such metallic nanoparticles to be structurally altered through chemical adsorption is increased; simplistically speaking, they are becoming easier to pull apart.

Further, naked metal particles will self organise in order to minimise surface free energy. This results in the formation of particles whose surfaces terminate in low index surface planes. Moreover, the three-dimensional structure representing the lowest energy configuration for the particle can be predicted from the Wulff construction and modifications of it.[10–12]† Fig. 3 shows an example of this.[9]

The relative proportions of low index facets, along with the interfaces that exist between them, change as a function of the size of the particle. Geometrically, these facets offer differing sites for adsorption, and have different propensities for reconstruction as a result of adsorption. As a range of planes co-exists within a single particle their interfaces may yield unique reaction sites with no "extended surface" analogue.[13] Further, the proximity of the planes to each other means that chemical exchange/communication can exist between them. As a result of this further complexity reactive behaviour can arise simply through changing the size/shape of a particle.[14]

Lastly, below a certain size limit the formation of well defined surface facets becomes progressively more limited and the reactive behaviour displayed by the metal in question may change completely as a result of a quantum size effect. As a result, a transition from "metallic" to "non-metallic" behaviour is also expected at some point.[15]

It is noteworthy that all the above can be deduced without even considering how adsorption or chemical reaction might perturb the energetic balance of the system and how that system might respond to such stimuli.

Fig. 4 shows a theoretical result that illustrates some of the subtle, and potentially reactively important ways in which free Au clusters respond to the molecular adsorption of CO.[16]

The calculations show that a molecular adsorbate can facilely manipulate the cluster to maximise the number of sites it would prefer to adsorb at. The result is a morphological rearrangement within the cluster that creates more four-co-ordinated Au sites: a flatter particle morphology and higher overall dispersion thus results.

How do we dynamically observe and quantify such phenomena?

As this review is primarily concerned with dynamic structural-reactive change, by and large, *ex situ* techniques wherein the sample under study needs to be removed from its working environment are not deemed to be of great utility. That said, some of the earliest and most important observations of, for instance, particle restructuring[17] and particle splitting/wetting in response to oxidation,[6,18,19] had, for reasons of the technology of the time, to rely upon this approach.

Latterly, however, developments in a variety of areas have resulted in a battery of advanced structurally direct and *in situ* techniques, and for the purposes of this review it is those that we shall principally consider. The reader is also directed to a recent review of a number of these techniques for more specific assessment of their current structural and temporal resolving powers.[20]

Obtaining atomic scale structural information requires probes of suitably small wavelengths. Thus the methods that

† In its original formulation[10] the Wulff construction applies to particles embedded within a single phase and at a fixed temperature. Supported metal nanoparticles which are not embedded interact—to varying degrees—with their support (and, indeed, the gas/liquid phases and the adsorbates that result from them). Thus the Wulff construction needs to be modified to take into account the presence of the interfaces between the particles and support and how deformable they may be in response to the contact with the nanoparticle. In the case of a non deformable boundary the modified Wulff construction due to Winterbottom[11] is more appropriate. However, subsequent treatments of this problem have shown that where metal–support contact can significantly deform the interfacial region further modifications to the treatment of the particle–support interface problems need to be adopted.[12]

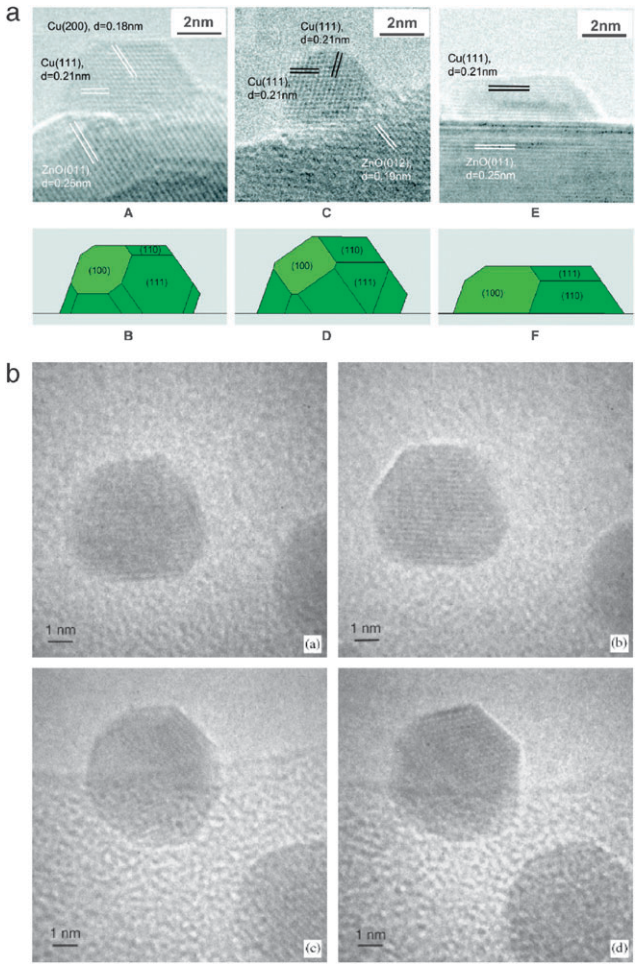

Fig. 5 (a) Top panels: *in situ* TEM from a Cu/ZnO catalyst at 493 K and as a function of environment: (A) 1.5 mbar H_2; (C) 1.5 mbar (3 H_2O : 1 H_2); (E) 5 mbar (19 H_2 : 1 CO). Bottom panels (B, D, F) show the corresponding Wulff constructions[10]† of the Cu nanoparticles. Reproduced with permission from ref. 21. (b) *In situ* TEM images of a single Au nanoparticle supported upon amorphous carbon in (a) vacuum; (b) under 2 mbar H_2; (c) under 2 mbar O_2; (d) again under 2 mbar H_2. Reproduced with permission from ref. 22.

may provide structurally incisive and dynamic information are those based upon electrons and X-rays: microscopies, diffraction, and techniques based upon absorption or scattering.

Foremost amongst the canon of microscopies that are of utility within the scope of this review are transmission electron (TEM) and scanning tunnelling (STM) microscopies.[20] Both of these techniques have developed to a very high level of sophistication, though the latter is constrained to planar systems rather than real high area materials.

Fig. 5a and b show two examples of the exceptional structural specificity that can be achieved on real systems and *in situ* using high resolution TEM.[21,22]

Both of the above examples clearly show that extremely precise investigation of nanoparticle (in these cases *ca.* 4–5 nm in diameter) structure and structural change can be achieved in "real" reactive environments. They clearly show subtle morphological rearrangements occurring as a result of interactions with adsorbates for two catalytically very relevant cases, *cf.* the theoretical results shown in Fig. 4. Moreover, the latest designs of these instruments also permit some ability to match these changes to some form of performance indicator such as activity/selectivity measured using a mass spectrometer.[20]

It does, however, need to be noted that in terms of the absolute pressures of gases used even the most modern of these instruments—and currently this can be said of STM as well—cannot operate at feedstock pressures really typical of many of the catalytic processes. In terms of direct relevance to what might be occurring in the real process, therefore, questions in this respect will always remain. However, and as with the pantheon of UHV studies, one cannot question the intrinsic beauty of the experiment, nor its contribution to a more fundamental understanding of how systems such as these behave in the presence of the gas pressures obtainable.

These examples provide *in situ* snapshots of nanoparticle structure but cannot, however, be regarded as "dynamic" within the paradigm of this article. Though "movies"‡ can be assembled from both TEM and STM experiments with varying degrees of time resolution, as with many other techniques, a concomitant loss of structure resolving power generally accompanies the increased temporal capacity.

Synchrotron based diffraction/scattering techniques and spectroscopies such as extended X-ray absorption fine structure (EXAFS) have also long been used *in situ* to study supported metal catalysts, and materials in general, to elucidate both long range and local structure respectively. Further, given suitable experimental design they are not, *a priori*, limited in the pressure regimes where they might be applied as is the case for electron based microscopies.

In terms of the lengths scales where these approaches find their most suitable application there is a very nice complementarity between EXAFS and both diffraction and electron microscopies. EXAFS is very much a local probe of structure and is very good at looking at systems wherein the species contain isolated metal atoms (for instance, surface organometallic species), small metal particles (with less than a few hundred atoms) or mixtures of oxidic/metallic material. It also has the significant benefit of being element specific.

However, EXAFS becomes rapidly and intrinsically less precise in relating co-ordination numbers to metal nanoparticle particle sizes and possible morphologies as the particles themselves get larger ($>$ *ca.* a few hundred atoms).[23] Fortunately, just as this is happening, diffraction and scattering probes are becoming more and more exact in their abilities in this respect.

Both EXAFS[24] and various diffraction based techniques have the potential to yield *in situ* and dynamic information, often with high time resolution. However, the literature would seem to indicate that in application to the study of the dynamic reactive behaviour of supported metal nanoparticles it has been the energy dispersive variant of the EXAFS technique that has, by a long way, found greatest application. In terms of time resolved diffraction or quick scanning EXAFS, the current pickings are rather scant in this arena.

‡ An *in situ* TEM "movie" of Pt particle redispersion can be found in the supplementary data of ref. 28.

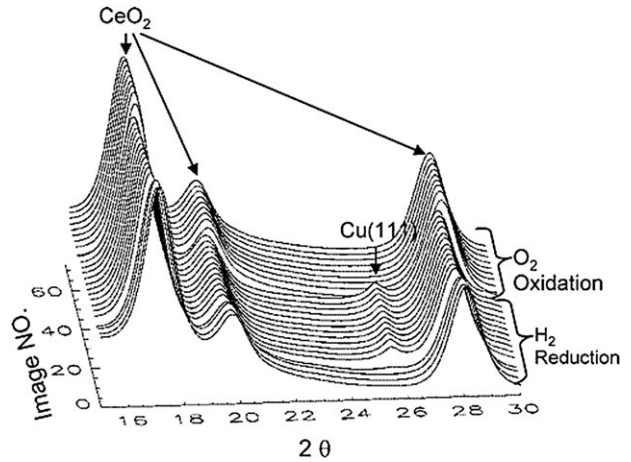

Fig. 6 X-Ray diffraction (λ = 0.922 Å) during redox treatment of $Ce_{0.8}Cu_{0.2}O_2$ at 573 K. The rapid removal of the Cu(111) reflection during the oxidising cycle is not accompanied by the formation of any observable CuO or Cu_2O. The Cu is switching between a solid solution within the mixed oxide and extruded Cu nanoparticles states on the oxide surface. Reproduced with permission from ref. 25.

Two exceptions that demonstrate the (largely untapped) potential for X-ray diffraction[25] and Quick Scanning XANES[26] are, however, worth noting. Both study the redox behaviour of Cu based catalysts for methanol synthesis and water-gas shift catalysis. The QEXAFS study[26] is most notable for the sheer speed of acquisition obtained (15 ms) for Cu K edge XANES and thus provides a clear demonstration of the potential that quick scanning variants of EXAFS might have in this arena.

Time resolved (1 spectrum min^{-1}) X-ray diffraction[25] concerning the reduction and oxidation of Cu within a mixed $CuCeO_2$ support is shown in Fig. 6.

Whilst relatively slow, the data obtained during *in situ* reduction and oxidation reveal a highly intriguing phenomenon: a rapid and reversible dissolution of supported Cu particles into the mixed oxide support which is not observed to occur in the simpler Cu/CeO_2 case. As we will see, this is not an isolated occurrence of this type of potentially useful behaviour.

It seems clear that the current sparsity of dynamic and high resolution experiments utilising the variety of microscopies, diffraction, and QuEXAFS techniques, and concerning the behaviour of supported metal nanoparticles, cannot last and we will return to consider this before the end of the review.

In the meantime, having delineated the types of structural change that one might observe in working catalyst systems, broadly discussed why they might be important, and what possibilities we have to study them directly, we now review some case studies. We will deal in detail only with the behaviour of the three metals most commonly associated with three-way car exhaust catalysts (Rh, Pd, Pt). Possibly as a result of their extensive application, and the intrinsically dynamic environment that exhaust catalysts work within, it is this grouping that provides the richest seam of currently available data. Moreover, within this grouping of metals examples of each type of behaviour (*e.g.* Fig. 1), and combinations of behavioural types, can be found.

Platinum based systems

Platinum has a hugely important and widespread usage: from hydrocarbon reforming and the cleaning up of car exhaust emissions, to application in fuel cell catalysts. It was from within the petrochemical industry that many of the perennial bugbears of many heterogeneous catalytic processes were first recognised: that of poisoning by sulfur, early research into which provided one of the first clear examples of adsorbed induced refacetting in metallic nanoparticles from static TEM;[17] and that of sintering—a loss of active surface area as a result of an increase in supported nanoparticle size.[5]

Noble metal redispersion, the rejuvenating antidote to its problematic cousin, has been known almost as long as sintering itself.[6,18] It has, however, been limited by factors that one would ideally want to avoid: it requires a high temperature oxidation step, and, historically has only been efficient—from an applied point of view—when Cl is used as an adjunct to the catalyst formulation or within the oxidation process itself. Through *in situ* and dynamic study, we are starting to uncover a lot more about both these processes and realise the possibility of redispersion in the absence of Cl; a

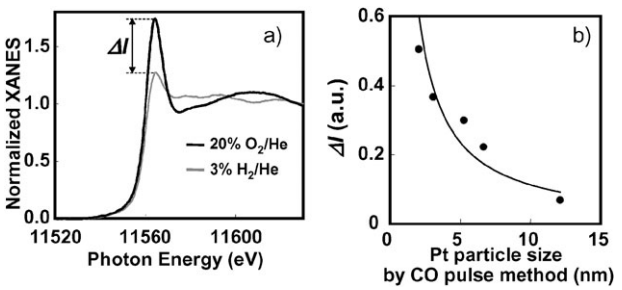

Fig. 7 (a) Pt L_{III} edge XANES collected using fluorescence yield dispersive EXAFS from a 2 wt% Pt sample maintained at 873 K under flowing 20% O_2–He or 3% H_2–He as indicated. Each spectrum is acquired in *ca.* 1 s. (b) Correlation of changes in Pt L_{III} "white line" intensity (ΔI) with Pt particle size as determined by pulsed CO chemisorption. Reproduced with permission from ref. 27.

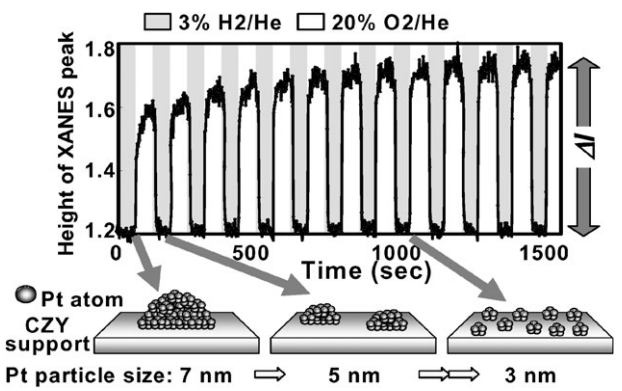

Fig. 8 Temporal variation of Pt L_{III} "white line" for a sintered Pt/CZY catalyst (initial average Pt particle size = 7 nm) during redox treatment (20% O_2–He gas and 3% H_2–He gas, 60 s each) at 873 K, and a schematic representation of the redispersion behaviour. Reproduced with permission from ref. 27.

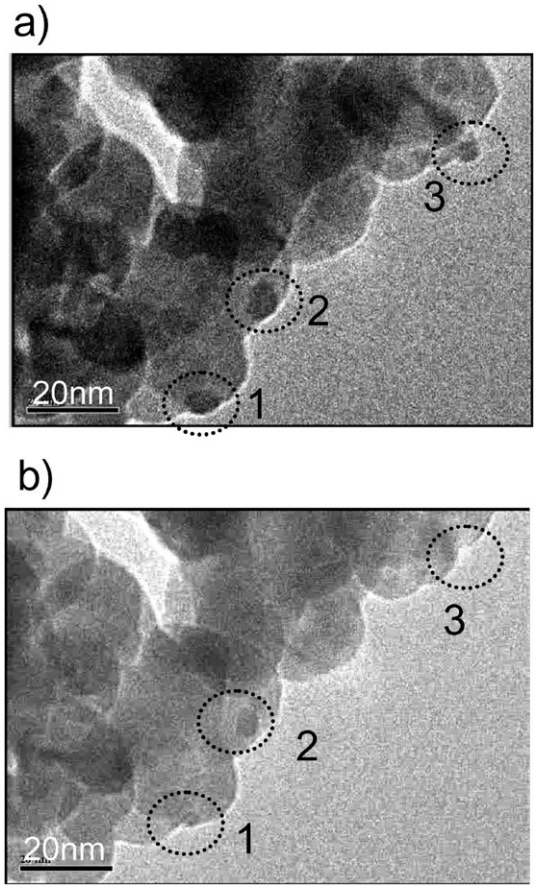

Fig. 9 *In situ* TEM‡ images for 2 wt% Pt/CSY at 1093 K. (a) Initially sintered catalysts with average particle size of 6 nm. (b) After exposure to 1.3 kPa O_2 for 480 s. Each of the circled Pt particles is seen to decrease in size or disappear completely during the oxidative treatment. Reproduced with permission from ref. 28.

goal that has the potential for extending the working life of car catalysts within their operational environment.

Fig. 7–9 summarise the results of recent studies in this direction carried out by Toyota. Their extensive research[27,28] has utilised a cross referencing of static measurements (EXAFS and TEM) combined with *in situ* fluorescence yield energy dispersive XANES. Through this combination of techniques a relationship between the Pt L_{III} edge "white line" height (ΔI) and the size of the supported Pt particles is suggested. Changes in this parameter can then be measured *in situ* using fluorescence yield dispersive EXAFS on a timescale of *ca.* 1 s. As such, and within the paradigms advanced, investigation of the dynamic character of chemically induced Pt sintering and redispersion results.

The results shown in Fig. 8 indicate that in certain cases (in this case Pt supported upon a support comprised of Ce, Zr and Y) a very considerable redispersion (from an average diameter of 70 Å) can be gradually achieved, toward an apparent limiting Pt particle diameter of *ca.* 30 Å. What is more, this method starts to tell us something about the kinetic nature of this process. The first oxidative cycle produces the largest redispersion. Subsequent oxidative cycles augment this initial redispersion, but to progressively smaller degrees. The process is also seen to be intrinsically rapid (occurring in a few seconds) and reversible, according to the feedstock being experienced.

This behaviour *is not observed* for equivalent Pt/Al_2O_3 catalysts,[28] showing that the structure and composition of the support material are crucial in determining the structural-reactive behaviour of the metal (*cf.* the Cu based example of Fig. 6 and further examples of behaviour in Pd based systems given below.)

Nor are these results consistent with simple "morphologically static" oxidation (be it surface limited or bulk) of the Pt (other possible interpretations of the observed changes in the Pt L_{III} XANES). A bulk oxidation process should show a parabolic rate law with fast oxidation of the outer layers followed by diffusion limited slow oxidation of the bulk of the particle.[29] Surface limited oxidation should show a phenomenologically similar kinetic profile. However, in both of these cases, an isothermal experiment would not result in the temporal changes observed in the intensity of the XANES feature from cycle to cycle.

However, whilst these EXAFS measurements can tell us much about the overall nature of the process they cannot tell us exactly how this process is occurring. To establish this, Toyota have turned to *in situ* TEM in both static and dynamic modes.[28] Fig. 9 shows quite conclusively that Pt is redispersed through what is known as "atomic migration" of PtO_x species as opposed to the particles being split into progressively smaller entities by the action of adsorbed O. The atomic migration model was proposed long ago on the basis of *ex situ* TEM[18,19] and finds its driving force in the surface limited formation of a PtO_x (or, in the presence of Cl, a PtO_xCl_y) layer. The strain induced between this thin oxidic layer and the remaining metallic core is proposed as a sufficient driving force for the "sloughing" of this layer and the transport of Pt over the support. It would appear that on its own the Al_2O_3 cannot stabilise the resulting PtO_x layer sufficiently, and therefore maintain the Pt redispersion. The CSY, however, can, leading to an efficient and Cl-free reversal of the sintering of the Pt.

Supported Rh systems

Relative to Pt, Rh is an intrinsically more oxophilic element displaying a much more diverse organometallic chemistry (most notably a rich variety of complexes with CO and NO). Both of these properties, and a simple deduction based upon the much lower cohesive energies of Rh relative to Pt (*cf.* Fig. 2) add even more potential for a variety of dynamic structuro-reactive behaviour on the nanoscale.

Within the reams of research regarding Rh catalysts, as with Pt, a great deal of attention has been paid to two basic conversions, *i.e.*:

$$2CO_{(g)} + O_{2(g)} \rightarrow 2CO_{2(g)} \quad (1)$$

$$CO_{(g)} + NO_{(g)} \rightarrow CO_{2(g)} + \tfrac{1}{2}N_{2(g)} \quad (2)$$

The first evidence that suggested organometallic aspects of its chemistry, rather than purely its metallic surface behaviour, might be important to its catalytic function came from the

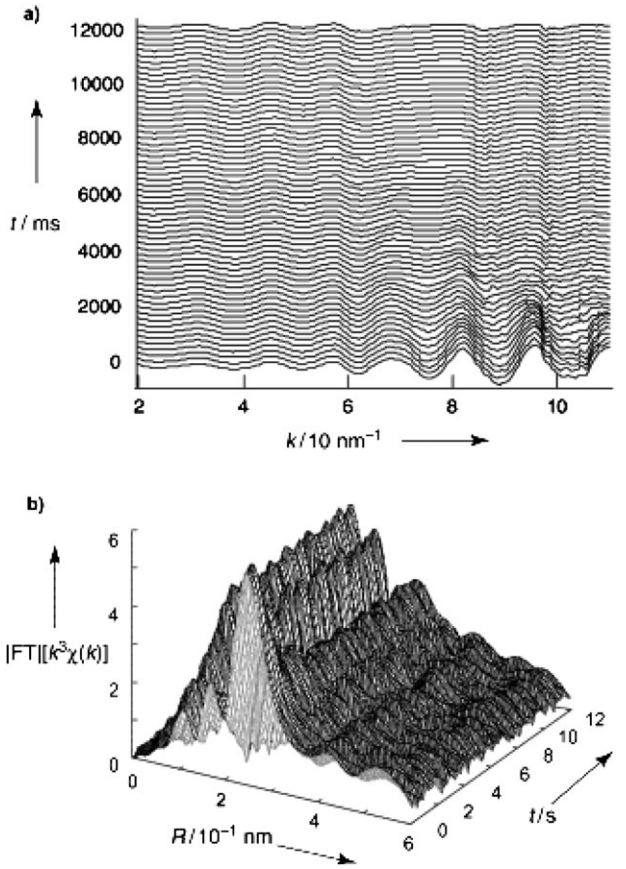

Fig. 10 (a) Rh K edge dispersive EXAFS, in k^3 weighted form, from a reduced 2 wt% Rh/Al_2O_3 sample during exposure to CO. (b) Fourier transform (FT) representations of the same data. The rapid loss of Rh–Rh bonding as a result of the CO adsorption is clearly seen in the diminution of the FT peak between 2 and 3 nm^{-1}. Reproduced with permission from ref. 31.

infrared studies carried out by Yang and Garland in 1957.[4] They found that, alongside CO vibrations indicative of linear and bridge bonded CO adsorbed on metallic particles, a further pair of absorption bands indicated the formation of isolated $Rh^I(CO)_2$ species. The first structural affirmations of the surface organometallic nature of the $Rh^I(CO)_2$ came from the EXAFS of Koningsberger *et al.*[30] Their pioneering work also indicated that there appeared to be particle size limitation

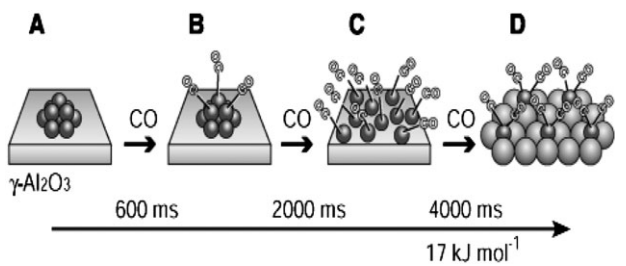

Fig. 11 A model of the oxidative redispersion of small supported Rh particles by CO derived on the basis of the dispersive EXAFS results and simultaneously acquired mass spectrometry. The transient formation of linear carbonyl species upon the small Rh particles is implied to act as the catalyst for their subsequent disruption into isolated $Rh^I(CO)_2$ species. Reproduced with permission from ref. 31.

to this "oxidative disruption": above a particle size of *ca.* 10–15 atoms the formation of the $Rh^I(CO)_2$ was ostensibly extinguished (*cf.* Fig. 2).

But how do species like $Rh^I(CO)_2$ form from nanoparticulate Rh? What are their structures, and what role might they have to play in, for instance, the two chemical conversions noted above? It was not until recently that a structurally direct technique, with a time resolution sufficient to see within some of these processes, was applied to their study.[31]

Fig. 10 shows results from transmission energy dispersive EXAFS studies made during the interaction of small supported Rh nanoparticles with CO. Fig. 11 summarises the structuro-reactive deductions made from them.

Firstly, the corrosion of small reduced Rh particles is very rapid indeed, with Rh–Rh co-ordination indicative of these particles being lost within *ca.* 2 s of exposure to CO; hence the correspondingly low apparent activation energy derived from the dispersive EXAFS measurements.[31]

Secondly, it is the initial adsorption and formation of linear carbonyl species that is proposed to drive the eventual collapse of the small Rh particles. The rapid accumulation of these species collectively withdraws electron density from the Rh until the cohesive energy of the small particle is compromised to the degree where formation of individual $Rh(CO)_2$ species becomes the energetically favourable option. This model is favoured over an alternative mechanism wherein $Rh(CO)_2$ species might form directly at sites of lowest Rh–Rh co-ordination (corner sites for example) and the Rh atom is subsequently extracted from the starting particle.

But what about the role of this phase change within a catalytic process? Structurally indirect infrared measurements have played a significant role in unravelling some of these questions: time resolved, concentration modulation infrared,[32] for instance, most elegantly establishing the "spectator role" of this species within catalytic oxidation of CO to CO_2 by O_2.

It is the case, however, that as spectator species go, the $Rh^I(CO)_2$ species is somewhat special—it is a spectator that actually contains an atom of the catalytically active metal component. As such one might ask whether it has any other role to play? Surely, if one forms more and more of this species there must be less and less Rh present in catalytically active forms to mediate the catalytic process at hand?

Fig. 12 shows further time resolved insight into this question, and indeed further aspects of this catalytic conversion from *in situ* dispersive EXAFS.[33] Here reduced 5 wt% Rh samples are subjected to 5% ($CO + O_2$)–He gas flows—of varying CO/O_2 ratio—before being heated in a quartz microreactor whilst EXAFS and mass spectrometry data are taken. Analysis of the EXAFS yields an average local Rh–Rh co-ordination number (N_I^{Rh}). In this case, and in tandem with observations of the near edge structure of the Rh EXAFS, it can be shown[33] that for CO/O_2 ratios ≥ 1, below the light off for CO conversion, significant amounts of the Rh are tied up as catalytically inactive $Rh^I(CO)_2$ species and significant conversion is only achieved once this has been transformed back to metallic Rh. Thus the facile liability of Rh nanoparticles in the presence of CO can become a significant factor in determining the efficiency of the catalyst for this conversion.[33] Moreover, in their initially reduced state the Rh

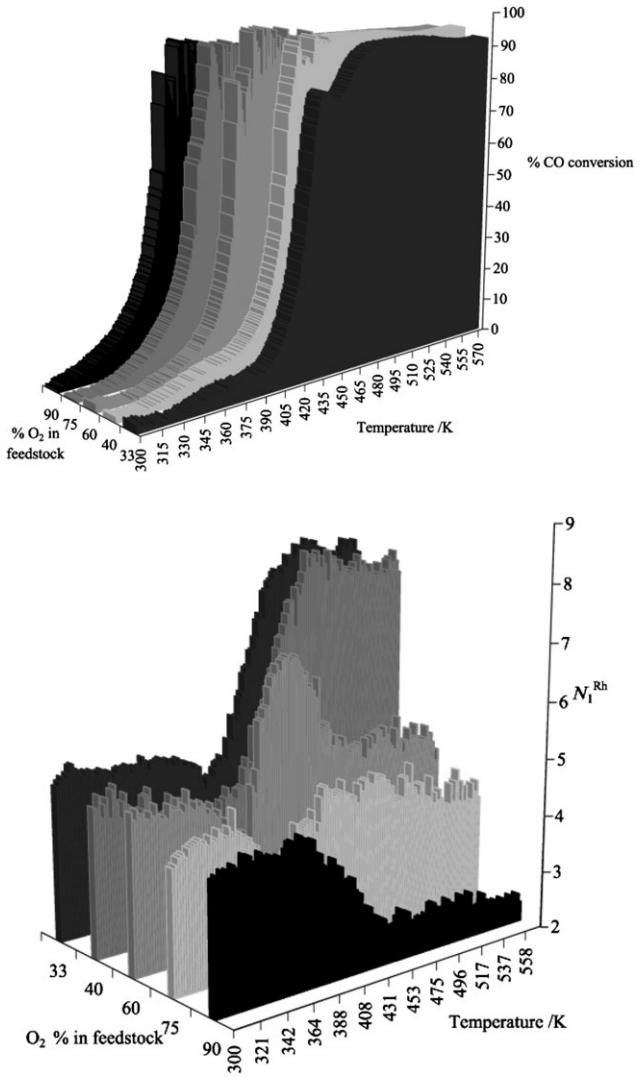

Fig. 12 Top panel: CO conversion to CO_2 over pre-reduced 5 wt% Rh/Al_2O_3 catalyst as a function of temperature and feedstock (CO–O_2) composition. Bottom panel: Rh–Rh first shell co-ordination (N_I^{Rh}) determined from Rh K edge dispersive EXAFS during temperature ramping to 573 K under the differing reaction mixtures. A N_I^{Rh} of *ca.* 7–8 is equivalent to that derived from the pre-reduced (under 5% H_2–He) sample. Reproduced with permission from ref. 33.

particles in this catalyst are, on average, *ca.* three times greater in size than the limiting size derived by Koningsberger *et al.* for oxidative disruption of Rh by CO alone.[30]

A further aspect of the structural-reactive behaviour of supported Rh nanoparticles is also revealed by this work. As the CO : O_2 ratio decreases below the stoichiometric condition (2 CO : 1 O_2) to $\ll 1$ the light off temperature for CO conversion drops. At the same time XANES/EXAFS indicates that the Rh phase present during catalysis is progressively oxidic (Rh^{III} rather than Rh^0 or Rh^I), even at very low temperatures. This implies three things: the first is that a highly oxidised Rh phase is very readily formed under such conditions; secondly that this oxide is actually the most active (lowest "light off" temperature) phase for CO conversion by Rh; and thirdly, that the local structure, and therefore reactive behaviour, of the highly dispersed Rh system can only be understood in terms of a dynamic equilibrium involving three phases of Rh *i.e.*

$$Rh^I(CO)_2 \leftrightarrow Rh^0 \leftrightarrow Rh_2^{III}O_3 \qquad (3)$$

The right hand side of this equilibrium has also been studied and is a good example of rapid, but apparently "morphologically static", phase change. Oxidation (by O_2) of *ca.* 11 Å diameter Rh particles[34] is well described by a parabolic rate law[20] and there is nothing indicative of significant spatial transport of the Rh during this process; a fact that appears to be borne out by high resolution electron microscopy from much larger Rh particles.[35]

A similar overall picture is emerging for NO reduction by CO.[36] However, this situation is again more complex. NO may dissociate and act as an oxidant. It can also form stable Rh nitrosyl species. However, an increased number of possibilities arise due to the extra electron that NO possesses relative to

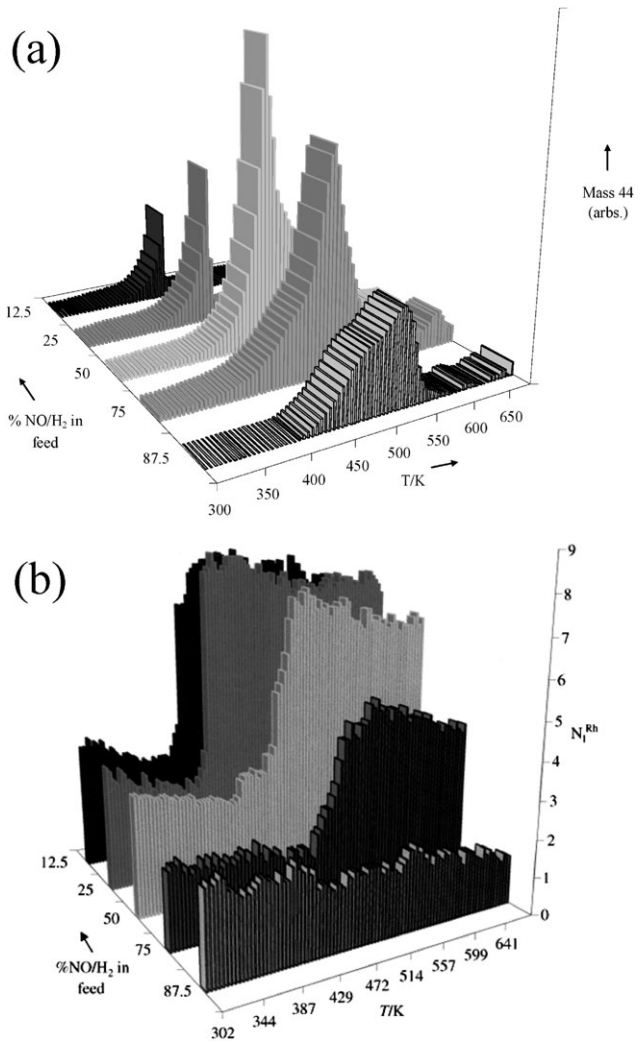

Fig. 13 (a) Selectivity toward N_2O during NO reduction by H_2 over 5 wt% Rh/Al_2O_3 catalysts as a function of temperature and feedstock composition. (b) Rh–Rh first shell co-ordination (N_I^{Rh}) from Rh K edge dispersive EXAFS during temperature ramping to 673 K under the differing reaction mixtures. A N_I^{Rh} of *ca.* 7–8 is equivalent to that derived from the pre-reduced (under 5% H_2–He) sample. Reproduced with permission from ref. 37.

CO. Thus, adsorption of NO to metallic Rh can have a variety of structuro-reactive consequences. Fig. 13 shows the relationship between the selectivity of NO reduction by H_2 as a function of the composition of the feedstock, temperature, and the nature of the supported Rh phase.[37]

In contrast to the observations made for CO oxidation by O_2 is the observation that light off for NO conversion decreases as the reaction feedstock is made more reducing. Appreciable amounts of N_2O are, for the most part, observed only *during* the transition of the Rh from oxidised to reduced states and in amounts that decrease with increasing H_2 content. Indeed, in the most oxidising conditions used no evidence for the formation of a metallic phase of Rh ever arises. Correspondingly, only a low level of NO turnover, that produces high levels of N_2O and that fizzles out to nothing at *ca.* 600 K, is observed.

A comprehensive study[38] of the interaction of NO with small metallic Rh particles has followed. Fig. 14 summarises the results obtained during 60 s of NO exposure to reduced Rh at a variety of temperatures. In this experiment infrared spectroscopy and dispersive EXAFS are applied synchronously with mass spectrometry with *ca.* 60 ms time resolution.

At 373 K NO adsorbs in a predominantly molecular manner (ν(NO) = 1680 cm^{-1}), practically no Rh oxidation occurs,

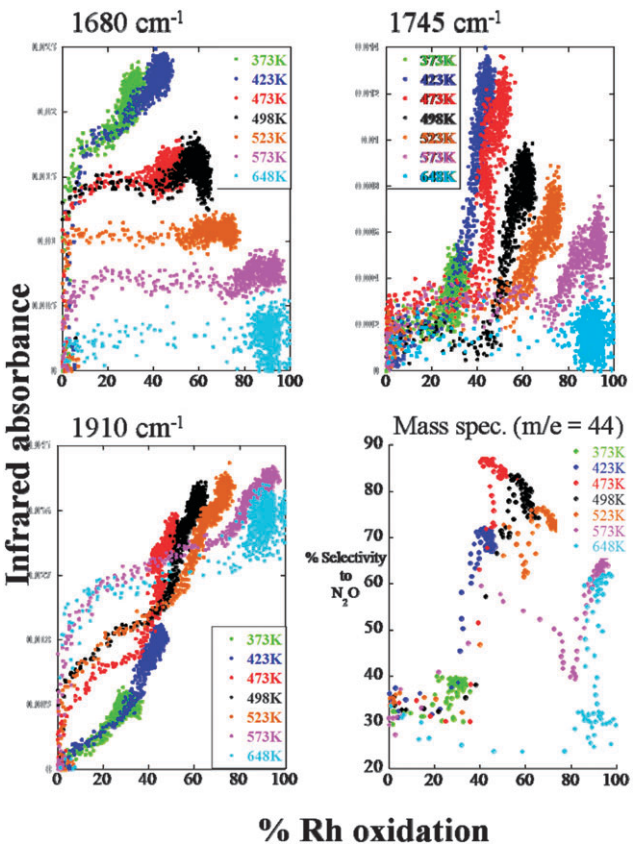

Fig. 14 Correlations between nitrosyl infrared bands (at the wavenumbers indicated), and the net selectivity of the interaction of NO, with the degree of Rh oxidation (from Rh K edge dispersive EXAFS). Results derived from exposing pre-reduced 5 wt% Rh/Al_2O_3 catalysts—average Rh particle diameter of 11 Å—to NO at the temperatures indicated. Reproduced with permission from ref. 38.

and Rh particles of this size largely resist oxidative disruption, retaining their native *fcc* structure. However, both the net Rh–Rh co-ordination falls and the average Rh–Rh bond length visibly increases (from 2.68 Å to 2.70 Å): the adsorbed NO molecules, it appears, are trying to pull apart the 11 Å diameter Rh particles. For these *ca.* 11 Å diameter particles they fail, but the changes in Rh–Rh co-ordination could be interpreted as indicative of the NO severely reshaping the Rh particles in a manner similar to that shown in Fig. 4.

However, if we decrease the starting particle size of the Rh to *ca.* 10–20 atoms (*ca.* 7–8 Å diameter)[39] large scale and rapid oxidative disruption to form $Rh(NO)_2$ (the nitrosyl analogue of $Rh^I(CO)_2$) is, at least in the first instance, observed.

Thus a highly significant change in the physicochemical properties of supported Rh nanoparticles occurs over a relatively small range of average particle size (between 8 and 11 Å diameter, *cf.* Fig. 3).

As the temperature is increased NO dissociation by the (initially) metallic Rh particles becomes increasingly dominant. This results in an increasingly fast oxidation of the Rh and a change in the types of NO species that are observed to be formed. By 573 K the only significantly IR observable species is linear $Rh(NO^+)$ at *ca.* 1910 cm^{-1}. This species can only form at oxidised Rh sites that have been rapidly created through NO dissociation. If we again reduce the starting size of the Rh particles to 7–8 Å diameter and repeat this experiment at 573 K, no differences in structural reactive behaviour are now observed.[39] *When rapid oxidation of the Rh dominates, size dependent differences in behaviour driven by molecular NO adsorption at lower temperatures disappear.*

A further IR visible nitrosyl species (a "bent" nitrosyl at 1745 cm^{-1}) only appears in between these two extremes—at indicative Rh particle stoichiometries of RhO_4–Rh_4O_3. At the same time the selectivity of the interaction to N_2O is maximal.[38] A direct relationship between the degree of Rh oxidation, the nitrosyl species formable upon differently oxidised phases, and the net chemistry that results may therefore be established.

Increasingly, at least in the case of highly dispersed Rh, the lively interplay between reduced, oxidic and surface organometallic phases during reactions such as these is being revealed. As a result the potential importance of such reactive phase change in determining catalytic light off, overall activity, and, perhaps most importantly selectivity, can be quantified and understood. As a last point we might also quite reasonably expect Ru—of importance in methanol fuel cell applications, for example—along with other metals displaying an extensive organometallic chemistry, such as Ir, to have a similar structural-reactive potential in the presence of gas such as CO and NO.

Supported palladium systems

As with Rh and Pt, Pd is applied in auto-exhaust catalysis but is also widely researched in many other areas such as methane oxidation and carbon–carbon coupling chemistry (Heck and Suzuki reactions, for example). In each of these areas of application the potential for reactive change in the structure

of the catalyst is of great interest: sintering and poisoning (and their avoidance) are ever present concerns but, in the case of Pd, the exact nature and relationships and interconversions between metallic and oxidic Pd have been very much centre stage. In liquid–solid phase conversions, such as Heck chemistry, leaching of surface bound Pd into the liquid phase (either as an organometallic or colloidal species) is yet another example of a structural-reactive process that has considerable applied importance—though one that has received little by way of detailed dynamic structural-reactive attention.

It has long been known that the oxidation of supported Pd nanoparticles is anything but simple or "morphologically static". The seminal *ex situ* TEM studies of Ruckenstein and Chen[19] showed as early as 1981 that oxidation of Al_2O_3 supported Pd nanoparticles is accompanied by an array of size dependent particle splitting and flattening phenomena.

The very recent application of X-ray diffraction using both conventional (10 keV)[40] and high energy (85 keV)[41] X-rays to model planar systems has started to probe Pd nanoparticle oxidation with a previously unaccessible structural specificity—one that can assess *in situ* the size of supported Pd/PdO nanoparticles but also their detailed morphology. This is possible due to the utilisation of a highly oriented substrate and the subsequent formation of truncated octahedral Pd particles with well defined (100) and (111) facets from which crystal truncation rods are clearly observable in the reflection XRD experiment. Moreover, a particularly elegant experimental strategy permits a further rapid determination of how particle size effects manifest themselves in this case.[41] Fig. 15 and 16 show aspects of the size dependent structural-reactive understanding that results.

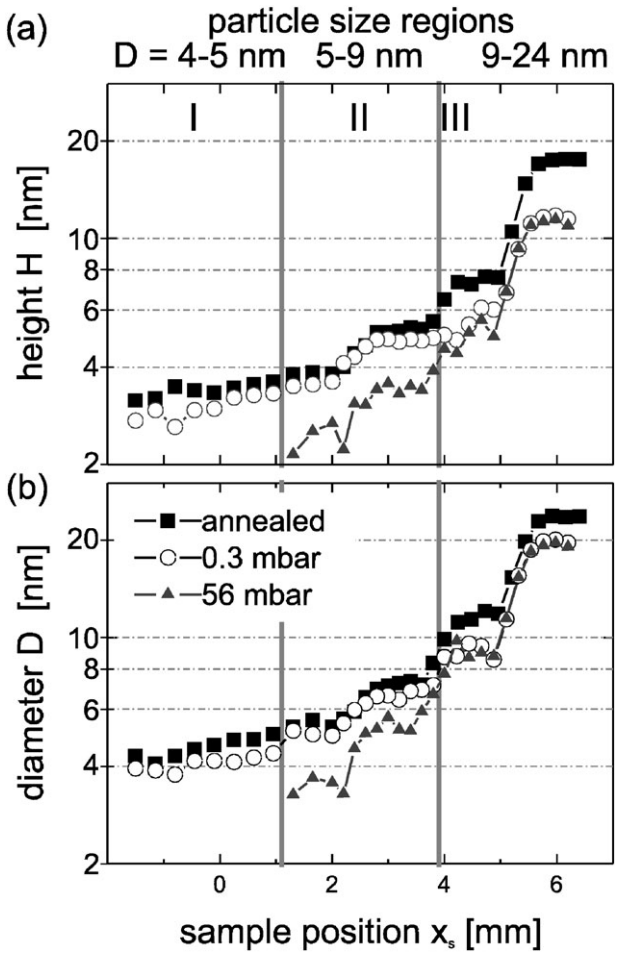

Fig. 15 Size dependent behaviour observed for the oxidation of Pd particles adsorbed upon MgO(100) at 570 K. (a) Particle height and (b) particle diameter as a function of treatment (as indicated). Three, size dependent, regimes of oxidative behaviour of the Pd nanoparticles are indicated (Roman numerals). Reproduced with permission from ref. 41.

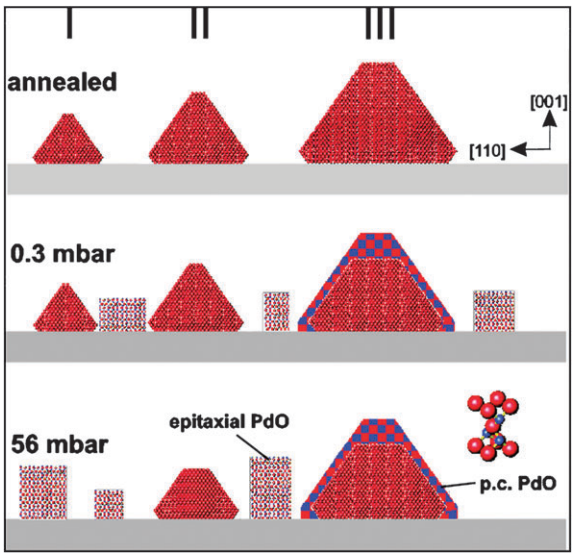

Fig. 16 Schematic illustration of the size and pO_2 dependent regimes of oxidation at 570 K, for Pd particles supported upon MgO(100). Derived from hard X-ray (λ = 0.14 nm) surface X-ray diffraction. Reproduced with permission from ref. 41.

Above 9 nm diameter an essentially "morphologically static" oxidation takes place that is self limited by the formation of a thin, passivating, layer of PdO which remains atop the remainder of the metallic Pd core. Between 5 and 9 nm particle size the oxidation process takes on a new character wherein a continual shrinkage of particle height and diameter is observed under 56 mbar O_2 and at 570 K. At the same time evidence for the growth of epitaxial (on the MgO substrate) PdO appears. Below *ca.* 5 nm Pd particle diameter, O_2 completely removes any evidence for metallic Pd within the timeframe (as low as 9 s per diffraction pattern)[41] of the experiments and only small domains of epitaxial PdO are observed.

It is clear that such a wide ranging and dynamic response to oxidation as a function of Pd particle size should have important ramifications as to the behaviour of real highly dispersed nanoparticulate Pd systems operating in net oxidising and/or "redox" conditions. As such, we now turn to some salient examples of what can happen in such real high area catalysts in situations that start to mimic in some ways the environmental fluctuations they might experience when in use as, for instance, car catalysts. Firstly, in studying the dynamic structuro-reactive response of 1 wt% Pd systems supported upon 10 wt% $ZrCeO_4/Al_2O_3$ during cycling between 5% CO–He and 5% NO–He at 673 K a rapid and

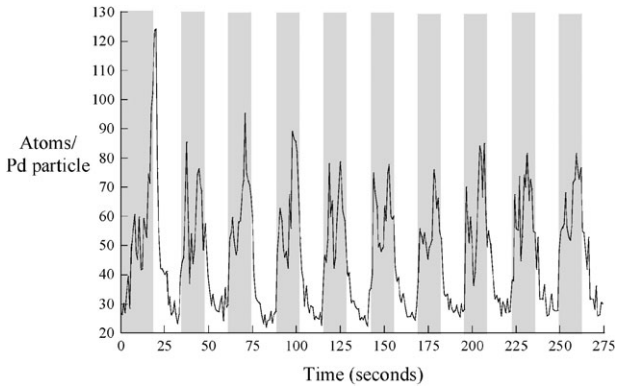

Fig. 17 Temporal variation in the apparent size during cycling between 5% CO–He and 5% NO–He at 673 K over a 1 wt% Pd/10 wt% $ZrCeO_4/Al_2O_3$ catalyst. Estimates of average particle atomicity are derived from analysis of dispersive EXAFS data collected at a 3 Hz spectral repetition rate. The shaded areas show the period under the reducing (CO–He) gas flow. Reproduced with permission from ref. 42.

reversible sintering (in CO–He) then redispersion (in NO–He) has been reported, and is shown in Fig. 17.[42]

During cycling between these two feeds, the average Pd–Pd co-ordination number (from EXAFS) was found to oscillate with the change in feed: under 5% CO–He it rapidly augments; in 5% NO–He it rapidly diminishes. To a first approximation[23] the average size of the Pd nanoparticles is rapidly changing in response to the environment it experiences. Importantly, we note that an extreme ''flattening'' of the nanoparticles cannot be explicitly ruled out on the basis of measurement alone (*cf.* the ''loss of height'' observed in the previous X-ray scattering studies[40,41] discussed above and the theoretical results shown in Fig. 4[16]). Either way, however, the dispersion of the Pd changes very rapidly under these redox conditions in the absence of any significant oxidation.

Subsequently the behaviour of 2 wt% Pd/Al_2O_3 was investigated during switching between CO and NO and CO and (5 O_2 : 1 NO) feed.[43] The results of this are shown in Fig. 18 for a single switch from reducing to oxidising conditions. This experiment shows firstly that the ceria–zirconia is not required for this structural reorganisation of the Pd to occur—in sharp contrast to the example of Pt sintering and redispersion given earlier. Secondly, the same behaviour is observed for rather larger Pd nanoparticles (in this latter case[43] up to *ca.* 3 nm in diameter). More surprising, however, was the result obtained by replacing the 5% NO–He feed with 5% (1 NO : 5 O_2)–He. The EXAFS derived Pd–Pd co-ordination data (left ordinal axis) are compared to the results of a Principal Component Analysis (PCA) of the XANES region (right ordinal axis); the latter quantifying the levels of Pd^{2+} formed during the redox cycle.

From these data we see that the presence of a large amount of oxygen in the oxidising feed actually promotes the degree to which the Pd particles are observed to flatten/diminish in size. Moreover, the majority of this structural change occurs before any substantive evidence of the formation of Pd^{2+} (*i.e.* formal oxidation of the Pd) can be derived.

As with the X-ray scattering measurements, two distinct—and, as it turns out, very rapid—processes appear to exist within the overall notion of Pd nanoparticle oxidation: a non oxidative, adsorbate induced, structural reorganisation that is then followed by a change in the phase of the supported metal (eventually to PdO).

This may be contrasted with the example given earlier regarding the behaviour of Pt catalysts within a more traditional paradigm of oxidative redispersion.[6,18,19] Within this paradigm the rapid formation of the oxide species itself is deemed to be the key event in redispersing the ''sintered'' Pt particles into much smaller entities. At least in the case of the high area Pd catalysts, any Pd oxidation observed under the conditions used in refs. 42 and 43 seems to be a secondary

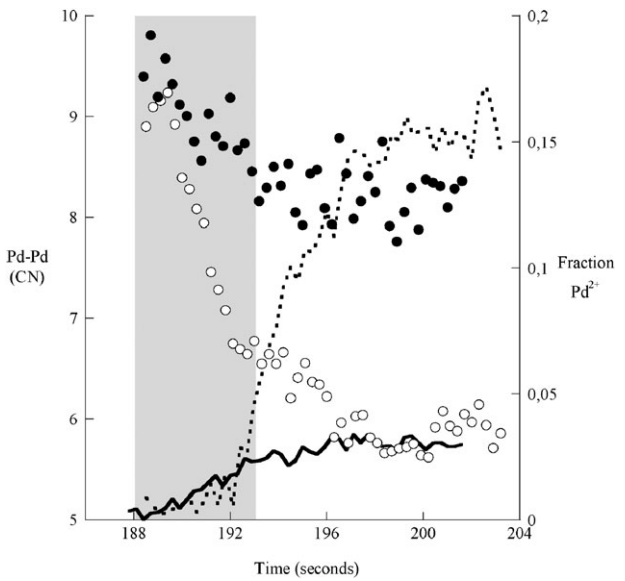

Fig. 18 Temporal variation in Pd–Pd co-ordination (from dispersive EXAFS analysis) and % Pd^{2+} (from XANES PCA analysis) observed within a single redispersion cycle. Solid circles/solid line = (5 O_2 : NO), open circles/hatched line = NO only. Within the shaded region, and with O_2 present, the Pd–Pd CN drops from *ca.* 9 to 6.5 within 2 s and with no obvious Pd^{2+} formation. Reproduced with permission from ref. 43.

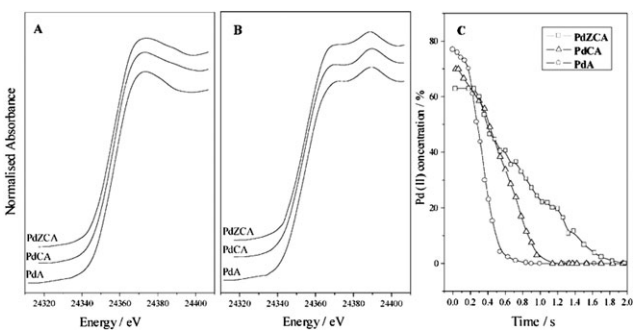

Fig. 19 (A) Pd K edge dispersive XANES spectra derived at 673 K from oxidised 1 wt% Pd supported upon Al_2O_3 (A), ceria–alumina (CA) and zirconia–ceria–alumina phases (ZCA). (B) Corresponding XANES derived from the samples after a brief reduction treatment. (C) The relative rates of reduction of Pd(II) to Pd(0) during the reductive cycle as a function of the support material. Reproduced with permission from ref. 44.

event that can account for only a minority of the redispersion of the Pd observed to occur.

In the above these rapid structural-reactive changes of Pd nanoparticles appear not to be affected unduly by the detailed nature of the support material, in contrast, it should be noted, to the examples (for Cu based catalysts[25]) given in Fig. 6, and the redispersion behaviour observed for Pt based catalysts shown in Fig. 7–9.[27,28] But what of the reduction behaviour of initially oxidic Pd species that might follow such events under more realistic—in terms of car catalyst function—changes in feedstock conditions?

Fig. 19 shows clearly how the nature of the support material can drastically affect the ability of oxidic Pd to be reduced to Pd nanoparticles during a reductive switch—in the presence of hydrocarbons—from a Lambda§ = 1.02 to Lambda = 0.98,[44] a compositional switch that is an accurate model of a change in engine operation from ''fuel lean'' to ''fuel rich'' conditions. What is evident is that (again) these sorts of events occur very rapidly and that the nature of the support material has a very significant bearing on events.

The overall speed of Pd reduction is close to five times slower for Pd on a 10 ZCA support compared to an Al_2O_3 support. The kinetics of the reduction process are also tangibly different. From the point of view of the catalysis at hand in these studies, this paper also shows that there is a considerable ''knock on'' effect regarding the ability of each catalyst to convert CO to CO_2 that follows as a direct consequence of their differing susceptibilities to reduction.

The ''intelligent'' catalyst: a structural-reactive redox solution to the problem of sintering

As has been stated, metal particle sintering has been a perennial bugbear in many catalytic processes, shortening the working lifespan of catalysts and, as a result, requiring the implementation of separate reactivation (redispersion) methodologies. A research group from Daihatsu has demonstrated new catalysts having a seemingly inbuilt resistance to sintering processes and, as a result, a much improved performance in certain types of auto exhaust application.[45,46] This catalyst is based upon a low surface area $LaFeO_3$ Perovskite, wherein part of the Fe component is substitutionally replaced by Pd (to yield, for example, $LaFe_{0.95}Pd_{0.05}O_3$). A combination of Anomalous Fine structure and EXAFS firstly established that when oxidised the Pd atoms occupy the (B) sites of the Perovskite structure (Fig. 20) and become part of the support structure itself.

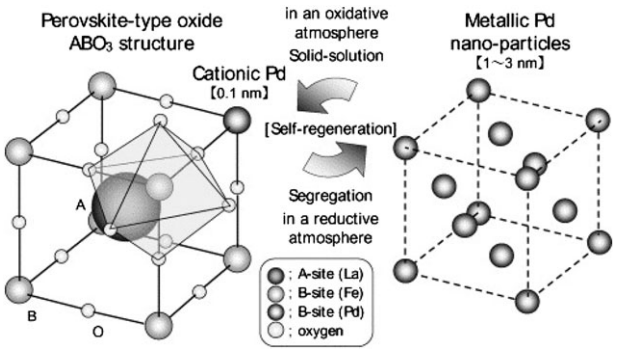

Fig. 20 Schematic diagram of the structural basis of the behaviour of the ''intelligent'' Pd Perovskite catalyst. In an oxidising environment the Pd may form an ultra dispersed solid solution within the framework Perovskite support material. Under reducing conditions it may switch from this state to form reduced *fcc* Pd nanoparticles residing at the surface of the support. Reproduced with permission from ref. 46.

§ Lambda cycling refers to the periodic and rapid (in ref. 45 at 0.6 Hz) oscillation of the feedstock composition above and below that deemed ideal to achieve maximal reduction of NO_x, and, in almost the same breath, maximal oxidation of CO and hydrocarbons to CO_2. As such for the structural reactive processes to be considered as candidates for improved catalytic performance under these conditions it should be demonstrated that they may actually act on sufficiently short timescales.

Reduction at high temperatures has the effect of pulling this framework Pd to the surface of the oxide whereupon it clusters to yield small Pd particles (*cf*. the diffraction based example of the behaviour of a $CuCeO_2$ catalyst given in Fig. 6).[25]

The hypothesis therefore became that the superior properties of this catalyst during testing procedures (Lambda cycling + ageing‡) compared to, for instance, Pd supported upon Al_2O_3, arose from the ability of the Pd to switch between these two states with such alacrity and efficiency that ''ripening'' and particle agglomeration simply cannot occur.

Yet again dispersive EXAFS[46] has been used to investigate this hypothesis, it being the only currently available structural technique with the potential temporal resolution to determine whether this was indeed the case. The results of such testing for the reduction (in pure H_2) cycles are shown in Fig. 21.

From these data it was firstly shown that observable differences in the rates of reduction of the Pd in the Perovskite and Pd/Al_2O_3 systems do indeed exist: the former being faster than the latter (though, as can be seen from Fig. 21, both events are very rapid indeed). Moreover, despite the Al_2O_3 providing an order of magnitude greater surface area for Pd dispersal than the Perovskite, the latter particles remained small after the principal reduction event, whereas the former continued to grow.

After equivalent doses (only six seconds) of reductant the Al_2O_3 particles were implied from the EXAFS to have grown to almost twice the size of those on the Perovskite support.

The structural-reactive redox comparisons are therefore: an oxidation of Pd to PdO followed by reduction and

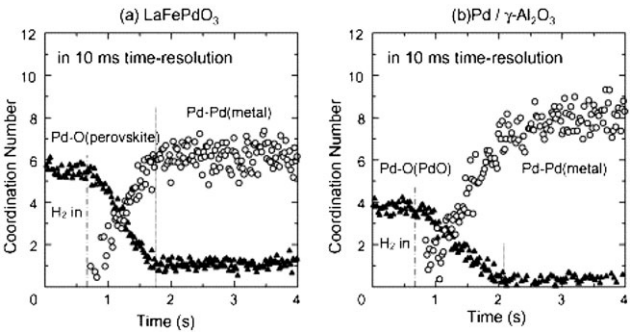

Fig. 21 Results derived from Pd K edge energy dispersive EXAFS showing the rapidity and extent for Pd particle formation during a switch to a reductive environment at 873 K, over (a) an ''intelligent'' Perovskite based catalyst and, (b) a simpler, Pd/Al_2O_3, catalyst of the same nominal Pd loading. Reproduced with permission from ref. 46.

ripening/agglomeration of the Pd metal particles on Al_2O_3; and, a novel structurally dispersive oxidation event followed by a reduction wherein ripening/sintering of the Pd particles is curtailed. That the metallic phase produced on the Perovskite should avoid these sintering processes points to a much higher heat of adsorption of the Pd on this material than on Al_2O_3; as the Al_2O_3 proffers 10 times the dispersing surface area of the Perovskite it would seem logical to conclude that the mobility of Pd particles or atoms in a reducing situation must be at least of the same magnitude greater on Al_2O_3 to achieve this effect.

Lastly, and importantly from an applied point of view, this same group has recently shown that this behaviour can be extended to both Pt and Rh versions of this catalyst.[46]

Summary and outlook

It seems only likely that given the continual refinement of structurally direct probes, and ever more powerful theoretical methods, that the sometimes subtle, sometimes gross, rearrangements that supported metal nanoparticles may undergo in response to adsorption and chemical reactions will become better understood. This will inevitably lead to a much more profound and incisive understanding of the manifold processes and applications they are used for.

Advances in various forms of microscopy, particularly STM[20] (which we have not dealt with in this review) and TEM, continue apace from both hardware and data processing perspectives.[20] This is leading to ever higher spatial resolution and potential for temporal resolution within elevated pressure "*in situ*" environments. Computational methods for restoring detailed structural information from the images these microscopies yield are also becoming more and more sophisticated and are leading to new experimental possibilities, especially for increasingly small nanoparticles.[47,48] The combination of advances on both these fronts promises much in respect of a heightened ability to investigate *in situ* structural-reactive change in nanoparticulate systems as it is occurring.

A similar state of affairs exists within the world of X-ray based techniques though, as stated earlier, many of the methods that could be brought to bear on these issues still await their full expression within the framework of the phenomena discussed in this review. Whilst time resolved EXAFS has been in the vanguard of *in situ* investigations of these phenomena its lack of precision in some circumstances requires that, in order to go further, techniques such as diffraction[20,49] and small angle X-ray scattering (SAXS)[50] on both powder and planar model systems need to be developed in this arena. There is already abundant evidence that these techniques have advanced to the state wherein coupling detailed *in situ* structural investigation with subsecond time resolutions is clearly now possible. One only needs to consider the surface X-ray diffraction work of Stierle *et al.*[40,41] shown here, along with others,[20] the SAXS work of Renaud[50] and co-workers, and recent developments in applying Pair Distribution Function (PDF) methods with high energy diffraction measurements[49] to see that the tools required to derive very detailed dynamic structural information on previously intractable systems, and within the dynamic paradigm of reactive processes, now exist and will only become more developed.

Conclusions

Supported metal nanoparticles are far from passive, immutable, entities that merely provide a surface based conduit for reactive chemistry and catalysis. Instead they are dynamic and flexible entities whose structures can actively react and respond to the environments that they experience. It is this inherent atomic scale structural flexibility and responsiveness that can ultimately determine the nature and efficacy of the chemical and catalytic processes that may result under a given set of conditions.

The heart of this behaviour is an often finely balanced game of energetics which may be driven in one direction or another by relatively small changes in the overall free energy of the system: changes that may be caused by, for instance, gas adsorption, desorption, chemical reaction, and/or changes in the metal/support adhesion energies.

We are now, courtesy of ever more structurally and temporally precise measurement, starting to recognise the potential importance of these diverse structural-reactive nanoscale possibilities. A much greater appreciation of how rapid, adsorbate induced, structural-reactive transformations might contribute to, or even dictate, the properties of nanosize metals systems within the environments wherein they are technologically applied is therefore starting to accrue.

However, the only thing that seems to be absolutely certain about this newly dynamic nanoworld is that we are only just at the beginning of fully comprehending it, and just how important these phenomena might be to a whole variety of existing and future technologies. It is an area that exists very much at the confluence of a number of disciplines: here the worlds of catalysis, classical surface chemistry and physics, surface organometallic and co-ordination chemistry collide. Each of these disciplines has its own history, liturgy, and viewpoint but it will only be through their effective braiding that a complete comprehension of these phenomena, and their practical ramifications, will emerge.

Acknowledgements

The author would like to thank the ESRF. Andreas Stierle (MPI, Stuttgart), Dominique Bazin (Université Paris-Sud), Yashihiro Iwasawa (University of Tokyo), Marcos Fernandez-Garcia (ISIC, Madrid), Naoyuki Hara (Toyota Motor Europe) and Yasutaka Nagai (Toyota Central Research and Development Laboratories) are also thanked for help and discussions regarding this article.

References

1 For instance: F. Besenbacher, I. Chorkendorff, B. S. Clausen, B. Hammer, A. M. Molenbroek, J. K. Norskov and I. Stensgaard, *Science*, 1998, **279**, 1912.
2 For instance: V. P. Zhadanov and B. Kasemo, *Surf. Sci. Rep.*, 1997, **29**, 35.
3 L. Mond, K. Langer and F. Quincke, *J. Chem. Soc., Trans.*, 1890, **57**, 749.
4 A. C. Yang and C. W. Garland, *J. Chem. Phys.*, 1957, **61**, 1504.

5 R. A. Dalla Betta, R. C. McCuney and J. W. Sprys, *Ind. Eng. Chem. Prod. Res. Dev.*, 1976, **15**, 169.
6 For instance: R. M. J. Fiederow, B. S. Chahar and S. E. Wanke, *J. Catal.*, 1978, **61**, 193.
7 C. T. Campbell, *Surf. Sci. Rep.*, 1997, **27**, 1.
8 D. Bazin, *Top. Catal.*, 2002, **18**, 79.
9 T. Lear, R. Marshall, J. A. Lopez-Sanchez, S. D. Jackson, T. M. Klapötke, M. Bäumer, G. Rupprechter, H.-J. Freund and D. Lennon, *J. Chem. Phys.*, 2005, **123**, 174706.
10 G. Wulff, *Z. Kristallogr.*, 1901, **34**, 449.
11 W. L. Winterbottom, *Acta Metall.*, 1967, **15**, 303.
12 E. J. Siem, W. C. Carter and D. Chatain, *Philos. Mag.*, 2004, **85**, 991.
13 For instance: V. P. Zhadanov and B. Kasemo, *Surf. Sci. Rep.*, 2000, **39**, 29.
14 V. Johanek, M. Laurin, A. W. Grant, B. Kaemo, C. R. Henry and L. Libuda, *Science*, 2004, **304**, 1639.
15 For example: M. Che and C. O. Bennett, *Adv. Catal.*, 1989, **36**, 55.
16 K. P. McKenna and A. L. Shluger, *J. Phys. Chem. C*, 2007, **111**, 18848.
17 P. J. F. Harris, *Nature*, 1986, **323**, 792–794.
18 E. Ruckenstein and Y. F. Chu, *J. Catal.*, 1979, **59**, 109.
19 J. J. Chen and E. Ruckenstein, *J. Catal.*, 1981, **9**, 254–273.
20 A. M. Molenbroek and A. Stierle, *MRC Bull.*, 2007, **34**, 1001.
21 P. L. Hansen, J. B. Wagner, S. Helveg, J. R. Rostrup-Nielsen, B. S. Clausen and H. Topsoe, *Science*, 2002, **295**, 2053.
22 S. Giorgio, S. Sao Joao, S. Nitsche, G. Sitja and C. R. Henry, *Ultramicroscopy*, 2006, **106**, 503.
23 A. Jentys, *Phys. Chem. Chem. Phys.*, 1999, **1**, 4059.
24 M. A. Newton, A. J. Dent and J. Evans, *Chem. Soc. Rev.*, 2002, **31**, 83.
25 H. Wang, J. A. Rodriguez, J. C. Hanson, D. Gamarra, A. Martinez-Arias and M. Fernandez-Garcia, *J. Phys. Chem. B*, 2005, **109**, 19595.
26 J. D. Grunwaldt, D. Lutzenkirchen-Hecht, M. Richwin, S. Grundmann, B. S. Clausen and R. Frahm, *J. Phys. Chem. B*, 2001, **105**, 5161.
27 Y. Nagai, N. Takagi, Y. Ikeda, K. Dohmae, T. Tanabe, G. Guilera, S. Pascarelli, M. Newton, H. Shinjoh and S. Matsumoto, *AIP Conf. Proc.*, 2007, **882**, 594.
28 Y. Nagai, K. Dohmae, Y. Ikeda, N. Takagi, T. Tanabe, N. Hara, G. Guilera, S. Pascarelli, M. A. Newton, O. Kuno, H. Jiang, H. Shinjoh and Shin'ichi Matsumoto, *Angew. Chem., Int. Ed.*, DOI: 10.1002/anie.200803126.
29 For example: R. E. Carter, *J. Chem. Phys.*, 1961, **34**, 2010.
30 H. F. J. Vant Blik, J. B. A. D. Banzon, T. Huizinga, J. C. Vis, D. C. Koningsberger and R. Prins, *J. Phys. Chem.*, 1983, **87**, 13.
31 A. Suzuki, Y. Inada, A. Yamaguchi, T. Chihara, M. Yuasa, M. Nomura and Y. Iwasawa, *Angew. Chem., Int. Ed.*, 2003, **42**, 4795.
32 M. Cavers, J. M. Davidson, I. R. Harkness, L. V. C. Rees and G. S. McDougall, *J. Catal.*, 1999, **188**, 426.
33 M. A. Newton, A. J. Dent, S. Diaz-Moreno, S. G. Fiddy, B. Jyoti and J. Evans, *Chem.–Eur. J.*, 2006, **12**, 1975.
34 M. A. Newton, S. G. Fiddy, G. Guilera, B. Jyoti and J. Evans, *Chem. Commun.*, 2005, 118.
35 For instance: G. Rupprechter, K. Hayek and H. Hofmeister, *J. Catal.*, 1992, **173**, 409.
36 M. A. Newton, B. Jyoti, A. J. Dent, S. G. Fiddy and J. Evans, *Chem. Commun.*, 2004, 2382.
37 M. A. Newton, A. J. Dent, S. Diaz-Moreno, S. G. Fiddy and J. Evans, *Angew. Chem., Int. Ed.*, 2002, **41**, 2587.
38 M. A. Newton, A. J. Dent, S. G. Fiddy, B. Jyoti and J. Evans, *Phys. Chem. Chem. Phys.*, 2007, **9**, 246.
39 M. A. Newton, A. J. Dent, S. G. Fiddy, B. Jyoti and J. Evans, *J. Mater. Sci.*, 2007, **42**, 3288–3298.
40 N. Kasper, A. Stierle, P. Nolte, Y. Jin-Phillipp, T. Wagner, D. G. de Oteyza and H. Dosch, *Surf. Sci.*, 2006, **600**, 2860.
41 P. Nolte, A. Stierle, N. Kaspar, N. Y. J. Phillipp, H. Reichart, A. Rühm, J. Okasinski, H. Dosch and S. Schöder, *Phys. Rev. B: Condens. Matter Mater. Phys.*, 2008, **77**, 115444.
42 M. A. Newton, C. Belver-Coldeira, A. Martinez-Arias and M. Fernandez Garcia, *Nat. Mater.*, 2007, **6**, 528.
43 M. A. Newton, C. Belver-Coldeira, A. Martinez-Arias and M. Fernandez Garcia, *Angew. Chem., Int. Ed.*, 2007, **46**, 8629.
44 A. Iglesias-Juez, A. Martinez-Arias, M. A. Newton, S. G. Fiddy and M. Fernandez Garcia, *Chem. Commun.*, 2005, 4092.
45 Y. Nishihata, J. Mizuki, T. Akao, H. Tanaka, M. Uenishi, M. Kimura, T. Okamoto and N. Hamada, *Nature*, 2002, **418**, 164.
46 H. Tanaka, M. Uenishi, M. Taniguchi, I. Tan, K. Narita, M. Kimura, K. Kaneko, Y. Nishihata and J. Mizuki, *Catal. Today*, 2006, **117**, 321.
47 L. Cervera, L.-Y. Chang, J. D. Crispin, D. Hetherington, A. I. Kirkland, D. Ozkaya and R. E. Dunin-Borkowski, *Angew. Chem., Int. Ed.*, 2007, **46**, 3683.
48 Z. Y. Li, N. P. Young, M. Di Vece, S. Palomba, R. E. Palmer, A. L. Bleloch, B. C. Curley, R. L. Johnston, J. Jiang and J. Yuan, *Nature*, 2008, **451**, 46.
49 P. J. Chupas, K. W. Chapman, G. Jennings, P. Lee and C. P. Grey, *J. Am. Chem. Soc.*, 2007, **129**, 13822.
50 G. Renaud, R. Lazzari, C. Revenant, A. Barbier, M. Noblet, O. Ulrich, F. Leroy, J. Jupille, Y. Borensztein, C. R. Henry, J.-P. Deville, F. Scheurer, J. Mane-Mane and O. Fruchart, *Science*, 2003, **300**, 1416.